RESEARCH ARTICLE

Bingzhong Chen · Kaoutar Boukamel ·
Joseph P.-Y. Kao · Birgit Roerig

Spatial distribution of inhibitory synaptic connections during development of ferret primary visual cortex

Abstract Intracortical inhibition in the primary visual cortex plays an important role in creating properties like orientation and direction selectivity. However, the development of the spatial pattern of inhibitory connections is largely unexplored. This was investigated in the present study. Tangential slices of layers 2/3 of ferret striate cortex were prepared for whole-cell patch clamp recordings, and presynaptic inhibitory inputs to pyramidal neurons were scanned by local photolysis of Nmoc-caged glutamate. Inhibitory synaptic currents (IPSCs) were first detected around postnatal day (P) 17. They originated locally around the recorded cells. Both the number and the total areas supplying the inhibitory inputs increased thereafter and peaked at the time around and shortly after eye opening (P29–37). A refinement period then followed in which the areas providing the majority of inhibitory inputs shrank from 600 μm around the recorded neurons to 200–300 μm in more mature animals ($\geq$P38). The amplitude of IPSCs increased progressively with increasing age. Long-range inhibitory inputs (>600 μm) were present around eye opening and they often developed into a clustered patchy pattern in more mature animals ($\geq$P38). In summary, our results show a refinement and clustering in the spatial pattern of inhibitory connections during postnatal development of ferret visual cortex.

Keywords Visual cortex · Ferret · Pyramidal cells · Inhibition · Development

B. Chen (✉) · K. Boukamel · B. Roerig
Department of Anatomy and Neurobiology, University of Maryland at Baltimore,
685 West Baltimore Street,
Baltimore, MD 21201-1509, USA
e-mail: broer001@umaryland.edu
Tel.: +1-410-7077397
Fax: +1-410-7062512

J. P.-Y. Kao
Medical Biotechnology Center and Department of Physiology,
University of Maryland at Baltimore, School of Medicine,
Baltimore, Maryland, USA

Introduction

The primary visual cortex is characterized by a columnar architecture in which neurons preferring similar stimulus features cluster to form functional domains (Hubel and Wiesel 1962, 1963; Shmuel and Grinvald 1996; Weliky et al. 1996). The selective response properties of visual cortical neurons have spurred many innovative experimental and theoretical efforts to understand the underlying synaptic circuitry (Sillito 1979; Sillito et al. 1980; Heggelund 1981; Berman et al. 1991; Bonhoeffer and Grinvald 1991; Woergoetter and Koch 1991; Somers et al. 1995; Ferster et al. 1996; Weliky et al. 1996; Crook et al. 1997; Roerig and Kao 1999). There is now overwhelming evidence indicating an important role for intracortical synaptic connections, and in particular intracortical inhibitory connections, in the generation of stimulus feature selectivity of visual cortical neurons (Sillito 1984; Martin 1988; Chapman and Stryker 1992; Eysel 1992; Berman et al. 1992; Vidyasagar et al. 1996; Roerig and Kao 1999; Roerig and Chen 2002). For example, it has been shown that connections between inhibitory neurons and excitatory neurons with similar (Woergoetter and Koch 1991; Berman et al. 1991; Somers et al. 1995; Roerig and Chen 2002) or orthogonal (Sillito 1979; Sillito et al. 1980; Heggelund 1981) orientation preferences sculpt the pattern of orientation selectivity. Similarly, converging inputs to excitatory cells from inhibitory neurons located in regions preferring similar and opposite directions appear to contribute to the emergence and sharpening of direction selectivity (Eysel et al. 1988; Crook et al. 1997; Roerig and Kao 1999).

Inhibitory connections are thus of tremendous functional importance. However, while there are numerous anatomical and electrophysiological studies focusing on the development of excitatory neurons and their patterns of connectivity (Rockland et al. 1982; Callaway and Katz 1990; Komatsu and Iwakiri 1991; Lubke and Albus 1992) and inhibitory (Albus et al. 1991; Komatsu and Iwakiri 1991; Kisvarday 1992; Albus and Wahle 1994; Azouz et al. 1997; Gao et al. 1999; Roerig and Chen 2002), very

little is known about the development of inhibitory connections. This is in part due to methodological limitations: interneurons are smaller, i.e., harder to record from, and fewer in number (less than 20% of cortical neurons). In addition, they represent a highly diverse group in terms of connectivity, molecular markers, and-nal properties (Kawaguchi and Kubota 1997; Beaulieu and Somogyi 1990) and show a wide range of morphological and physiological diversity.

Sensory experience during the postnatal critical period is essential for the normal maturation of visual cortical circuits and function (Hubel and Wiesel 1962). Although most studies have been devoted to the modification of excitatory circuits (Rittenhouse et al. 1999),there are indications that GABAergic circuits also change (Winfield 1983). Indeed, one hypothesis is that the maturation of inhibitorycircuits plays an important role in timing the critical periodfor the modifications of excitatory connections (Kirkwood and Bear 1994; Hensch et al. 1998; Huang et al. 1999). Evidence for the slow cortical maturation of inhibitory mechanisms derives primarily from anatomical studies. In rodents, the numbers of inhibitory synapses (Blue and Parnavelas 1983;Miller 1986) and levels of GABA-synthesizing enzymes increase until postnatal week 5 (Huang et al. 1999). Inhibitory circuits continue to mature after birth in the visual cortex, and there is a dramatic postnatal increase in the number of GABAergic inputs converging onto layer II/IIIpyramidal cells. These findings indicate that the GABAergic circuitry in the visual cortex is plastic and can be shaped by experience.

The spatial distribution and potential developmental refinement of inhibitory connections in the developing visual cortex has so far not been investigated. The present study was designed to examine the spatial patterns of inhibitory inputs to layer 2/3 pyramidal neurons in the developing visual cortex of the ferret, an excellent model system for studies of the developing visual system. Ferrets are born relatively immature as compared with other species, such as cat and rat (Luskin and Shatz 1985), which makes it an ideal model for developmental studies. Inhibitory inputs were recorded in tangential slices by whole-cell patch clamp recordings combined with laser scanning photostimulation (Katz and Dalva 1994). We addressed the following questions: (a) Does the spatial distribution of inhibitory inputs change during development and is there evidence for a patchy distribution of inhibitory synaptic connections resembling that of horizontal excitatory connections in layer 2/3? (b) Does a developmental refinement or rearrangement of inhibitory input patterns correlate with the onset of visual experience? This would indicate that the refinement of inhibitory connections is involved in the refinement of cortical maps and response properties of cortical neurons.

Materials and methods

All animal procedures were performed in accordance with the animal care and use guidelines of the NIH, with the approval of the Institutional Animal Care and Use Committee.

A total of 34 animals were used. Animals were divided into four age groups based on developmental stages. These age groups were P7–16 (before thalamic fiber ingrowth, 12 animals), P17–28 (before eye opening, ten animals), P29–37 (around eye opening, seven animals), and P38 and beyond (after eye opening, five animals). A total of 98 neurons in layer 2/3 of the primary visual cortex were recorded successfully from 81 slices. Of these, 54 neurons were identified morphologically as pyramidal cells based on dendritic and axonal morphology. The remaining cells were either nonpyramidal neurons or could not be found in histological sections. Only recordings from pyramidal neurons were analyzed. The number of cells in each age group was: P7–16, 18 cells; P17–28, 16 cells; P29–37, 12 cells; P38 and above, 8 cells.
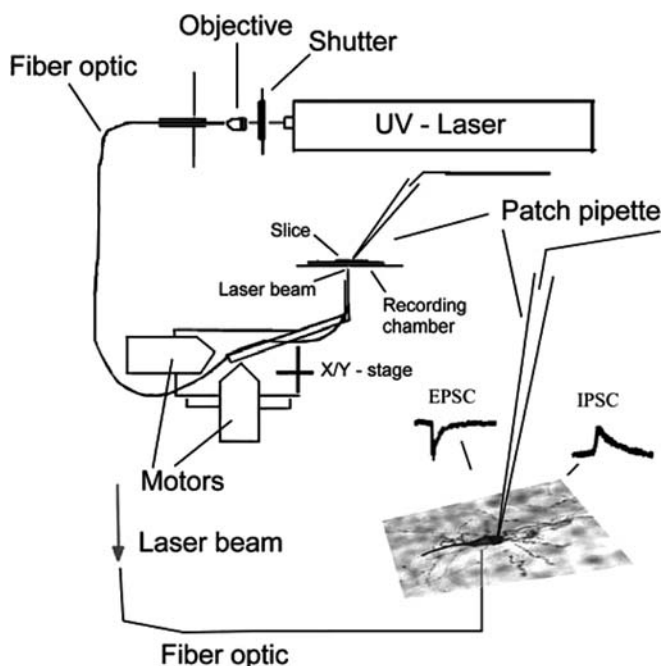
Slice preparation

Ferrets (P7 to adult, Marshall Farms, New Rose, NY) were deeply anesthetized with Nembutal (100 mg/kg, i.p.). Animals were then decapitated and blocks of tissue containing the primary visual cortex (area 17) from both hemispheres were removed. The block was placed into chilled standard artificial cerebrospinal fluid (composition: 125 mM NaCl, 5 mM KCl, 1.25 mM KH$_2$PO$_4$, 1.3 mM MgSO$_4$, 3.2 mM CaCl$_2$, 10 mM dextrose, 25 mM NaHCO$_3$) oxygenated with a mixture of 95% O$_2$ and 5% CO$_2$. Tangential slices (400 μm thickness) of area 17 were prepared with a vibratome and were maintained at room temperature in a chamber containing standard ACSF for 1 h before use. Slices containing layer 2/3 were used for patch clamp recording.

Patch clamp and photostimulation

Individual slices were transferred to a recording chamber mounted on the stage of an upright microscope (BX50WI, Olympus Optical, Tokyo, Japan). Slices were continuously superfused with standard ACSF oxygenated with a mixture of 95% O$_2$ and 5% CO$_2$ at room temperature. Electrophysiological recordings from single neurons were performed using standard whole-cell patch clamp methods. Patch electrodes (5–10 MΩ) were filled with internal solution (110 mMD-gluconic acid, 110 mM CsOH, 11 mM EGTA, 10 mM CsCl, 1 mM MgCl$_2$, 1 mM CaCl$_2$, 10 mM HEPES, 1.8 mM GTP, 3 mM ATP, pH 7.2) and 0.5% Biocytin (Sigma) was added. Voltage clamp recordings were conducted using a Warner PC-501 amplifier (Warner Instrument Corp. USA). Recordings were filtered at 1 kHz and digitized at 8 kHz. Resistances ranged from 11 to 17 MΩ, and a 30–50% compensation was usually achieved

using the amplifier adjustments. Synaptic inputs to the recorded neurons were scanned by local photolysis of Nmoc-caged glutamate, which was applied to the bath solution once a stable recording had been established (see details in Roerig and Chen 2002). This chemical was designed to resist spontaneous hydrolysis while yielding reasonable photorelease and kinetics (Rossi et al. 1997). Upon photolytic uncaging, light-induced cleavage of Nmoc-caged glutamate (on a sub-millisecond time scale) occurs followed a subsequent light-independent, pH-dependent decarboxylation (on the millisecond time scale). Because of the possible difference among animals of different ages in terms of ability to drive presynaptic cells to fire action potentials, a high concentration of Nmoc-caged glutamate (1 mM) was used to increase the firing probability. An argon/krypton ion laser (Spectra-physics Stabilite 2017) was used as a UV light source for local uncaging. The laser beam was coupled into a 50-μm-diameter fiber optic mounted to a motorized XY-stage. The fiber was moved within an oil droplet below the recording chamber. The laser beam was manually focused into the middle of the slice preparation (Fig. 1). Opening of the external shutter, scanning of the laser beam, and data acquisition were controlled by a National Instruments AD board (AT-MIO/AI E-10) and custom-written software (Labview, National Instruments).

The acquisition period for each laser stimulus (flash) was 1 s and the interstimulus interval was 3–5 s. In each acquisition period (1,000 ms), the shutter op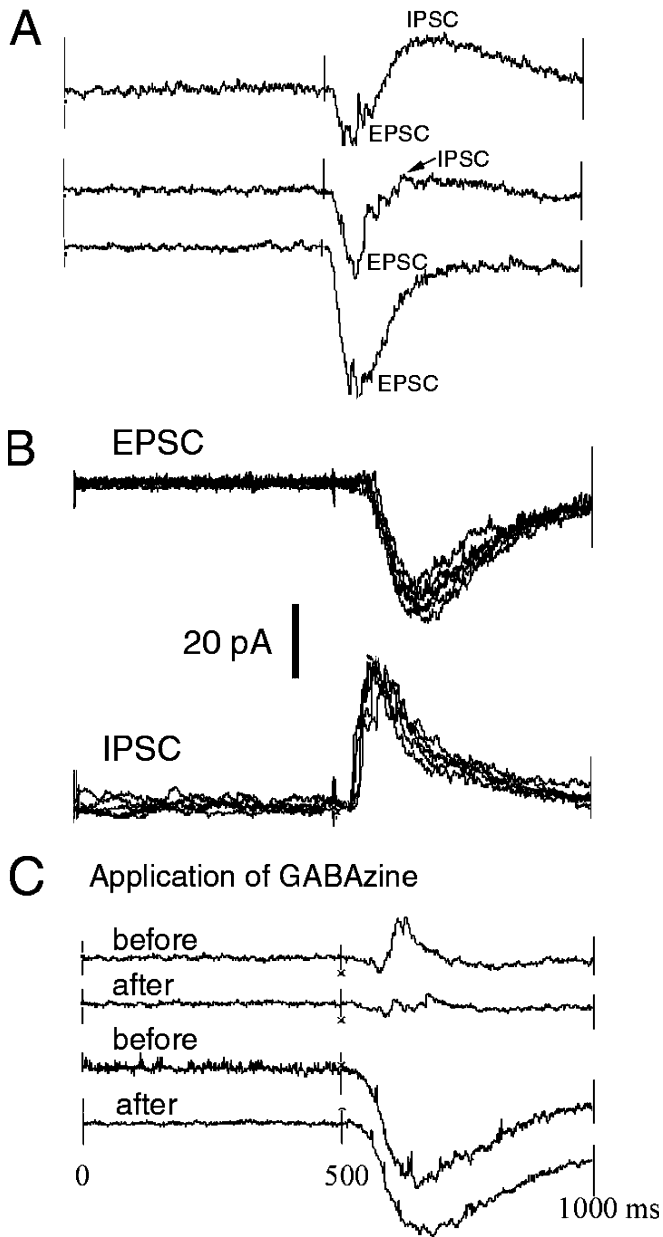ening occurred at 500 ms and the laser flash duration was 10 ms. The prestimulus acquisition period of 500 ms before shutter opening served to monitor spontaneous synaptic inputs to the recorded neurons. The spacing of stimulation sites was 50 μm. Typical maps consist of 500 to more than 2,000 stimulation sites, with sampling done in a "four-pass" mode, i.e., only every fourth spot was stimulated during one round and the map was filled in during four acquisition cycles.

The holding potential for the patch clamp recording was set at −20 mV to distinguish between excitatory and inhibitory synaptic inputs (Katz and Dalva 1994). At this holding potential, the outward inhibitory currents occurred as upward deflections (inhibitory postsynaptic currents: IPSCs) whereas inward excitatory events occurred as downward deflections (excitatory postsynaptic currents: EPSCs). Since most cells would fire and escape voltage clamp at this very depolarized holding potential, QX314 (100 μM) was added to the internal solution to block sodium channel. Depending on the stimulation site, either EPSC alone or IPSC alone or a mixture thereof could occur (Fig. 2A,B). IPSCs were almost abolished after bath application of GABAzine, a GABA$_A$ antagonist (Fig. 2C). In the photostimulation maps shown in the Results, only IPSCs are represented since our focus was on inhibitory maps. The current detection threshold was defined as 2x standard deviation. Direct photostimulation of the post-synaptic cell body resulted in spiking or a large, short-latency (~8 ms) inward current. In most cases, direct currents can be easily distinguished from postsynaptic currents by their short latency and large amplitude. Fig. 3 shows such latency differences. Direct activation had short latencies (mean 8.1 ms, standard deviation 2.45 ms, n=324 traces), whereas postsynaptic currents had much longer latencies (mean 55 ms, standard deviation 15.61 ms, n=7,561 traces). To further distinguish between direct activation and postsynaptic currents, tetrodotoxin (TTX, 1 μM) was added to the bath solution in two experiments to block synaptic transmission. In these cases, postsynaptic currents (EPSCs and IPSCs) were blocked while direct activation remained unaffected. In each slice only one to two cells were recorded to facilitate alignment and unambiguous assigning of input maps to postsynaptic cells.
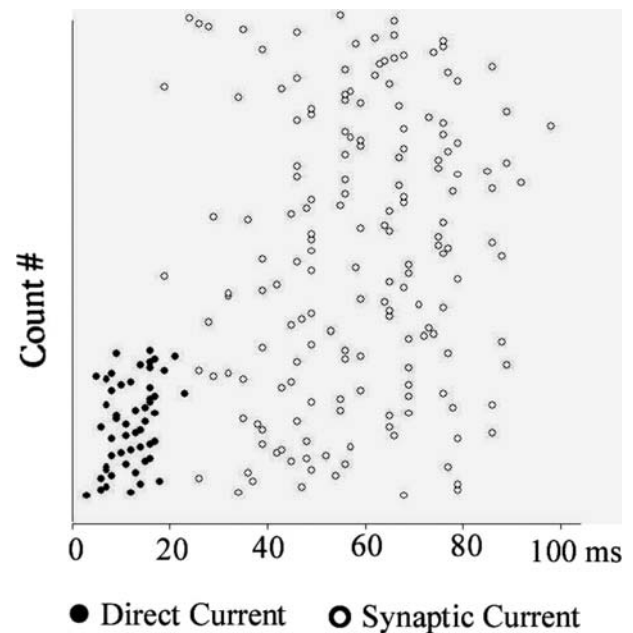
To test the consistency of the evoked currents, the same spot was photostimulated repeatedly. Figure 2B (upper traces) shows an overlay of five EPSCs evoked by stimulation of a presynaptic site repeatedly. No significant differences were observed among traces in terms of latency, amplitude, or peak time of the evoked currents. A similar result was found for IPSCs, as shown in the lower traces in Fig. 2B. Evoked currents were still reproducible with an interval of 30 min between stimulations of the same site. In addition, very similar maps were obtained from one cell in repetitive mapping experiments during a recording period of up to 2 h.

Fig. 1 Schematic representation of the photostimulation setup. The laser beam was coupled into a 50-μm-diameter fiber optic mounted to a motorized XY-stage. The fiber was moved within an oil droplet below the recording chamber. Synaptic inputs were scanned at 50-μm spacing. The duration of the shutter opening was 10 ms. Inhibitory and excitatory currents were separated by recording at a holding potential of −20 mV

A

B

C

Fig. 3 The distribution of onset latency for direct activation (*solid circles*) and synaptic currents (*blank circles*)

Fig. 2 A Different types of postsynaptic currents were evoked depending on the site of photostimulation. *Upper and middle traces* show mixed EPSCs and IPSCs. The *lower trace* shows an EPSC. **B** Consistency of evoked EPSCs (*upper traces*) and IPSCs (*lower traces*) when the same presynaptic site was stimulated repetitively, with an interval of 3–5 ms. In both examples there was little variation in current onset latency, amplitude, or duration. **C** Currents evoked by photostimulating the same sites before and after bath application of GABAzine. The IPSC was almost abolished after GABAzine application (*upper traces*), whereas EPSC was little affected (*lower traces*)

Histology

Following the recording session, slices were fixed for 1 day in 4% paraformaldehyde in phosphate-buffered saline (pH 7.4) and then transferred into phosphate-buffered saline solution containing 30% sucrose. Slices were resectioned at 70 µm on a vibratome and processed for

immunohistochemical visualization of biocytin-filled cells using a standard avidin-biotin (Elite) kit and DAB as chromagen. Labeled cells were inspected for identification of their cell type. Sections containing labeled pyramidal neurons were photographed for later alignment with photostimulation maps.

Data analysis and image alignment

All data shown here are from layer 2/3 pyramidal neurons. Before patch clamp recording, a slice overview image (including the position of the micropipette) was taken using a SONY XC-75 CCD camera and a SNAPPY (play) video frame acquisition module in conjunction with SNAPPY software. This slice image was used to aid the alignment of histological sections with synaptic input maps obtained by photostimulation (Fig. 4). The position of the stained postsynaptic cells in the histological sections and the direct activation area in the photostimulation map served as additional marks. The alignment was made using the layer menu of Adobe Photoshop. Only linear scaling and rotation were applied to images during alignment.

Photostimulation data were analyzed using custom software written in LabVIEW (National Instruments). Current events were inspected and manually marked. Only synaptic currents with onset occurring within 100 ms after shutter opening were selected for further analysis. This time window was determined based on our current clamp data showing that all photostimulation-evoked action potentials in presynaptic neurons occurred within this time frame (Roerig and Chen, unpublished). For each inhibitory current event, the delay to onset latency and peak amplitude was manually detected. The number and amplitude of spontaneous events in each trace were also

Fig. 4 Slice preparation and photostimulation. **A** Plane of sectioning for tangential slices. Only sections through layers 2/3 were used in our experiments. **B** Tangential slice through the upper layers prepared from a P48 ferret. The section contains the biocytin-filled postsynaptic cell. **C** Higher power view of the recorded (postsynaptic) layer 2/3 pyramidal cell. **D** Example of a stimulated ("mapped") area overlaid on a histological section of the recorded slice (here from a P35 animal). A live slice image was used to aid the alignment. **E** Morphology of another biocytin-labeled pyramidal neuron recorded in a tangential slice. The photostimulation map of this neuron is displayed in **F**. Each colored square in **E** corresponds to an area of 50×50 µm. The various colors are used to represent the amplitude of synaptic input to the recorded cell, as indicated by the color bar
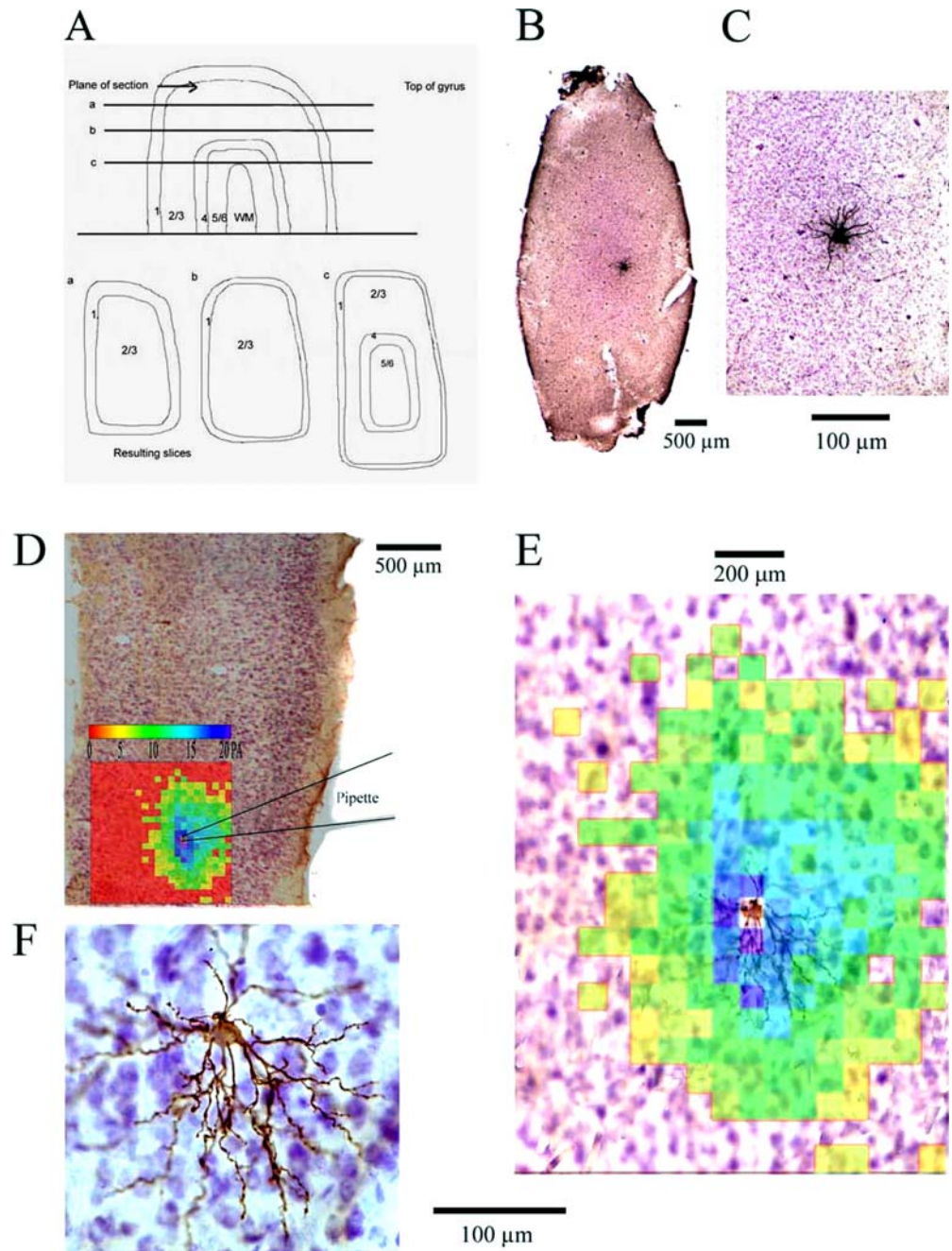
analyzed for later calculation of normalized synaptic input values (Dantzker and Callaway 2000). The analyzed data were then fed into a second program in which the selected events and their corresponding positions from which they were evoked were retained. This program yielded a photostimulation map in which the peak amplitudes (not the average amplitude) of current events were color-coded for each stimulation site. The current amplitude shown in this map was not corrected for spontaneous activity and differences of series resistance between each recording session. However, these two factors were taken into account when the overall synaptic input values were calculated, as described below.

To compare the spatial distribution of inhibitory inputs for each age group, the area surrounding the recorded cell was divided into concentric annuli spaced 200 µm apart. A normalized evoked input (NEI) value was calculated for each annulus of each recorded cell to compensate for differences in spontaneous events and series resistance among different recording sessions (Dantzker and Callaway 2000). For each annulus of 200 µm, the normalized input values NEI were calculated:

$$\text{NEI} = \frac{\overline{f_E}\,\overline{a_E} - \overline{f_C}\,\overline{a_C}}{\overline{a_C}}$$

where f_E is the mean number of evoked events, a_E is the mean amplitude of evoked currents, f_c is the mean number of spontaneous events and a_c is the mean amplitude of spontaneous currents.

The calculated values of the corresponding annuli from each cell of the same age group were then pooled and averaged. Plotting of histograms as well as statistical comparison of distributions was done using Sigmastat and Sigmaplot (Jandel).

Results

The main purpose of this study was to examine the spatial pattern of intracortical inhibitory connections in developing ferret visual cortex. To this end, the locations around the recorded neurons were scanned using the photostimulation method. A synaptic input map for each recorded neuron was thus obtained. These maps were color-coded, representing the amplitude of evoked currents. We defined local inputs as those PSPs elicited within 400 µm from the target cell. Those that originated at between 400 and 600 µm and at >600 µm were defined as intermediate and long-distance inputs, respectively. Results are described in the order of ascending age groups.

Early development before thalamic fiber ingrowths (P7–16)

At the early stage of this group, evoked currents mostly originated from a small area (within ~250 µm) around the recorded neurons. The majority of these currents resulted from direct activation of the recorded cell. Figure 5A shows results from a P7 ferret. The upper panel shows a color-coded map with numbered squares. The corresponding current traces for these numbered squares are displayed in the lower panel. Stimulations of the soma of the recorded cell (white square) evoked a short-latency (10 ms), large-amplitude (25 pA) direct activation (trace 1). This inward current had a flat plateau lasting for a few hundred milliseconds. This type of long-lasting direct current was characteristic of pyramidal neurons during the first two postnatal weeks. Similar current traces but with longer latencies were also observed (traces 2–4). They resulted from photostimulation of the dendritic trees of the recorded neuron. EPSCs could also be evoked at this early age from areas close to the cell body (within ~250 µm). However, they were usually of small amplitude (8–10 pA, trace 5) and were usually intermixed with and masked by direct activation. The amplitudes of direct activation and excitatory synaptic currents increased with age. Figure 5B shows a representative example from a later stage (P15) of this group. As compared with P7 (panel A), direct activation (trace 1) and EPSCs (traces 2–5) increased in amplitude and EPSCs were evoked from a larger area.

Fig. 5 Representative examples (**A** P7, **B** P15) from the P7–16 age group showing the results from photostimulation. For each panel, the color-coded photostimulation map is shown *at the top* and the current traces for the numbered squares on the maps are shown *below*. The *white square* marks the location of the recorded neuron. In **A**, evoked events originated from the area 200–250 µm around the recorded cell. Most of them represented direct activation. The direct activation in young animals (P7–P12) usually lasted for more than 500 ms. Small amplitudes of EPSCs (*trace 5*) were also observed. No IPSC was encountered. In **B**, the excitatory synaptic input (EPSC) map is shown *at the top*. Direct activation (*trace 1*) was evoked by stimulation of the recorded cell directly (*white square*). *Traces 2–5* show representative examples of EPSCs resulting from stimulation of multiple presynaptic sites. No IPSCs were detected
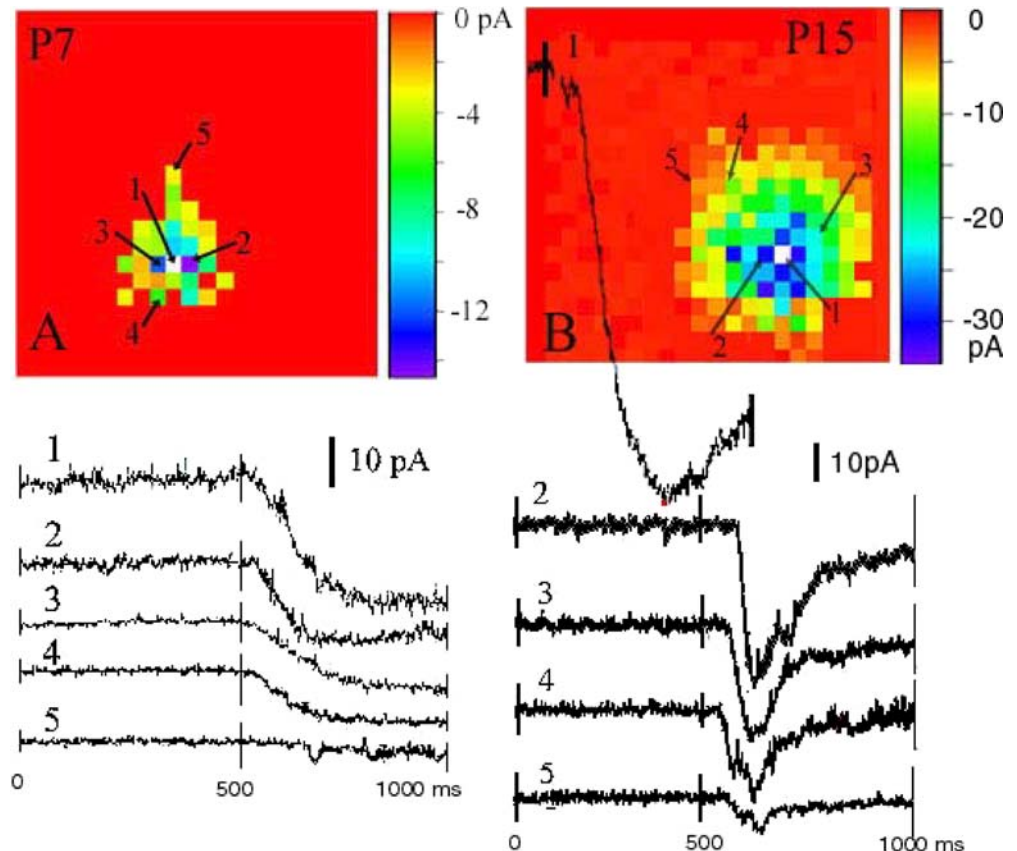
IPSCs, on the other hand, were not detected at P7. Even in more mature animals, IPSCs were not observed in most cases. In some cases, one to three small IPSCs (<8 pA) were recorded. Their paucity prevented us from generating a meaningful synaptic input pattern. Thus, at this developmental stage, while excitatory connections were already forming, a discernible pattern of inhibitory connections was not observed.

Age group before eye opening (P17–28)

A recognizable pattern of inhibitory inputs was first detected at P17. At this age, IPSCs were evoked from a small region (within ~200–300 μm) around the recorded cell (Fig. 6A). Their amplitudes were also small (maximum 15 pA). As age increased, both the number of presynaptic sites and the amplitude of IPSCs increased (Fig. 6B, P22; 6C, P28). At P28 (Fig. 6C), the region providing the majority of inhibitory inputs expanded to an area of ~500 μm distance around the recorded neuron. However, as the color-coded maps indicate, presynaptic sites closer to the recorded neurons usually provided stronger inputs to their target cells. In addition, IPSCs evoked from a similar distance away from the recorded cells usually had similar amplitudes. Long-distance inhibitory inputs (>600 μm) were rarely seen. These results suggest that inhibitory inputs were undergoing a constructive phase at this age group.

Age group around eye opening (P29–37)

Figure 7 shows results from representative examples of this age group (panel A, P30; panel B, P35). As seen in panel A (P30), the previous constructing phase of inhibitory connections continued and reached a peak at around P30–32. At this postnatal age, the area supplying the vast majority of inhibitory inputs further extended into a larger area of 600 μm around the recorded cells. The amplitude of IPSCs also increased as compared with those in the previous age group. In addition, long-distance inhibitory inputs (>600 μm) were present. However, they were few in number and patches of presynaptic sites generating IPSCs were rarely seen (panel A).

Fig. 6 Representative examples showing inhibitory synaptic input pattern recorded from the age group before eye opening (A P17, B P22, C P28). Inhibitory synaptic inputs (IPSCs) were first detected at the age of P17 (A). The IPSCs were evoked by stimulation of a small region (~200 μm) around the recorded cell and their amplitude was small. With increasing age, the number of effective stimulation sites increased and the average IPSC amplitude increased (B, C)
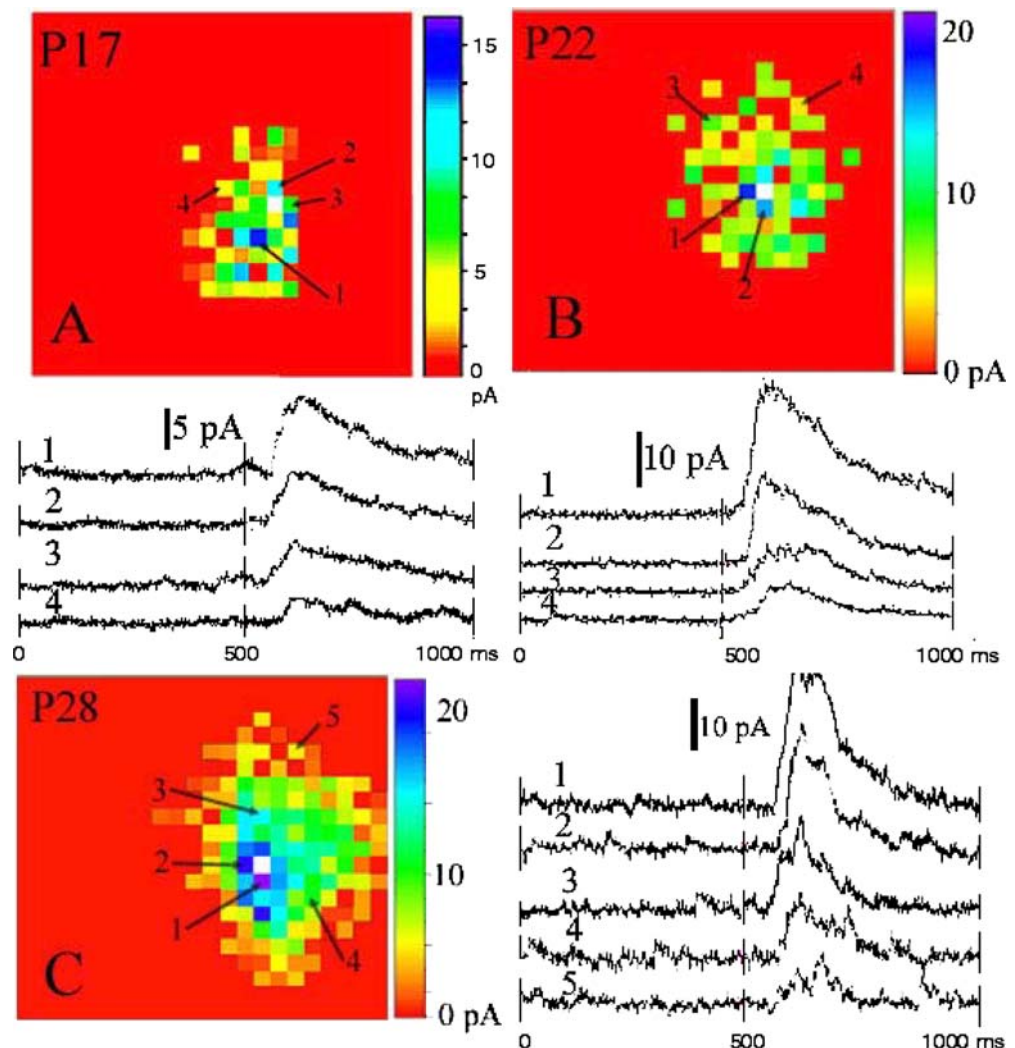
Fig. 7 Representative examples demonstrating inhibitory synaptic input maps from an age group around the time of eye opening (**A** P30, **B** P35). At the early stage of this group (P30, **A**), the majority of local inhibitory inputs originated from an area ca. 600 μm around the recorded neuron. At the late stage of this group (P35, **B**), the effective stimulation sites shrank to an area ca. 300 μm around the recorded cell. In addition, long-distance inhibitory inputs (>600 μm) appeared, although in small numbers. As compared with the previous age group, the amplitude of these local IPSCs increased
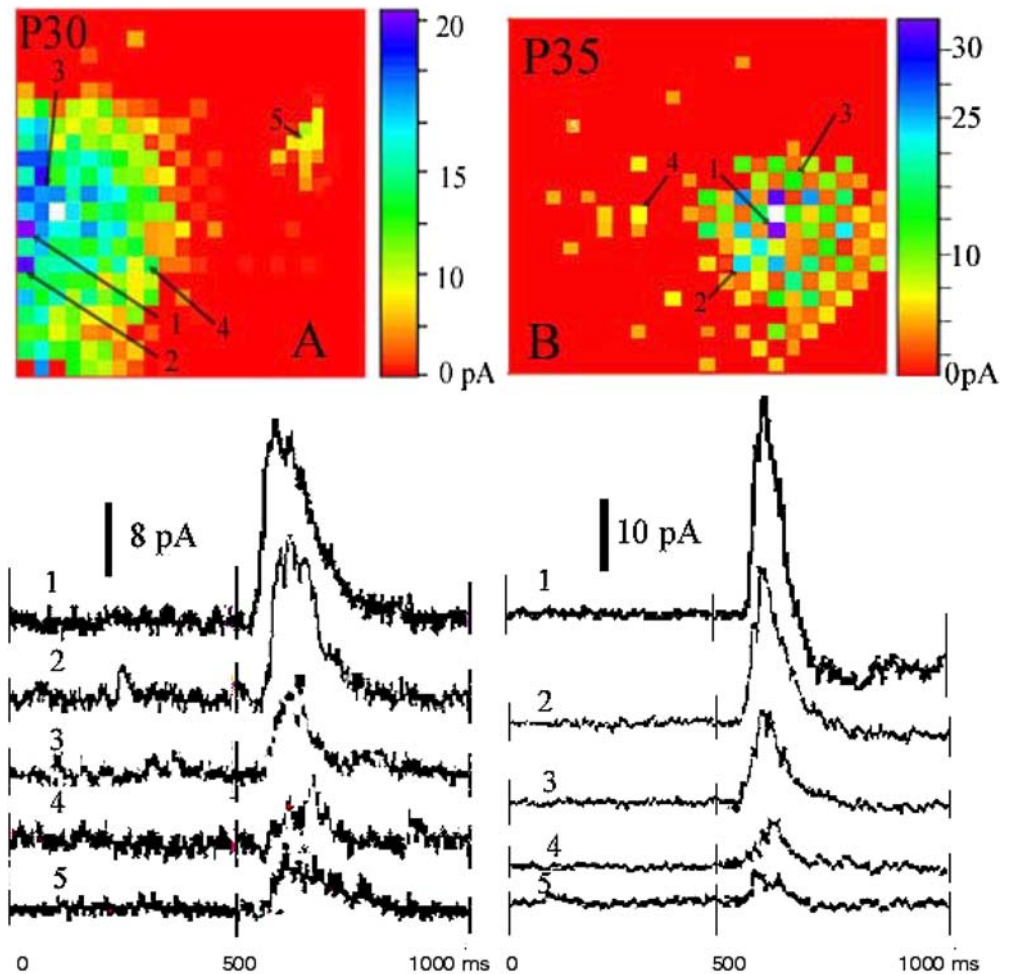
At the late stage of this age group, as seen in panel B (P35), the constructive phase of inhibitory connections appeared to pass into a rearrangement or modification period. This is indicated by the fact that the number of intermediate inputs (400–600 μm) began to decrease. In addition, IPSCs evoked from a similar distance from the recorded neuron showed a greater variation in amplitude (compare P35, Fig. 7B, with P28, Fig. 6C), indicating rearrangement or modification of synaptic inputs. Concurrent with these changes, the amplitudes of the inhibitory inputs (0–400 μm) increased, suggesting more efficient and/or more stable connections. The number of long-range inhibitory inputs also increased. Thus, around the period of eye opening, the intracortical inhibitory connections undergo an early constructing phase and a later rearrangement or modification phase.

Age group after P38 (after eye opening)

Figure 8 shows results from representative cases of this age group (panel A, P38; panel B, P56). Compared with the previous age groups, the area supplying the majority of inhibitory inputs decreased from ~600 μm to 200–300 μm (panel B) from the recorded neuron. The average ampli-

tude of these local inhibitory inputs, on the other hand, increased progressively as the animals became more mature. Thus, while the total number and areas supplying inhibitory inputs decreased, the potency of local inputs increased, indicating increased input specificity. Long-distance inhibitory inputs (>600 μm), while not commonly seen in the age group around the period of eye opening (P29–37), were encountered frequently in this age group. More distant inhibitory inputs up to 2 mm could also be found (panel B). Distant inputs tended to form a clustered pattern. On average, each cluster consisted of three to eight effective stimulation sites. IPSCs from the same cluster usually exhibited different kinetics, signaling that they originated from close but different presynaptic sites. It should be noted, however, that although the number of long-range inhibitory inputs increased as animals became more mature, their total number and average amplitude were much lower than those of the local inputs.

Quantitative comparison of inhibitory inputs among different age groups

Results from different age groups were compared by calculating the average amplitude of IPSCs and the

Fig. 8 Representative examples of inhibitory synaptic input maps recorded from the age group after eye opening (**A** P38, **B** P56). The presynaptic sites providing local inhibitory inputs shrank further to an area about 250 μm around the recorded neuron in the adult (**B**), while the IPSC amplitude increased. Long-distance inhibitory inputs increased in number and some of these presynaptic sites aggregated to form a clustered patch pattern. Note that the amplitude of long-distance inhibitory inputs is much smaller than that of the local inputs
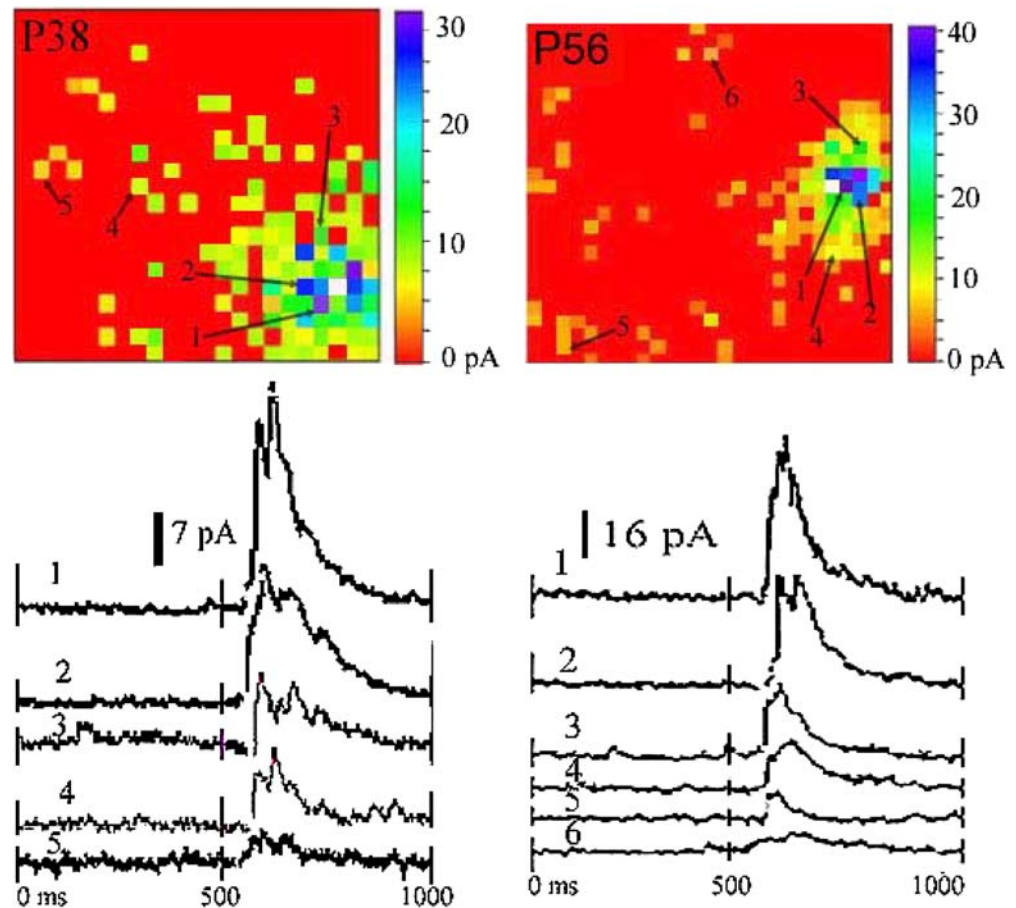
average percentage of effective stimulation sites. This was accomplished by pooling IPSCs elicited from the same distance range (at the interval of 200 μm) and from the same age group. A comparison of the percentage of effective stimulation sites (sites responding/total number of stimulation sites) is shown in Fig. 9, and a comparison of mean amplitudes is shown in Tables 1 and 2 and Fig. 10. As is evident from Fig. 9, most IPSCs originated from within 200 μm from the recorded cell in all age groups. In this distance range, there was no statistically significant difference among the groups. However, at the 200- to 400-μm range, the P29–37 group differed significantly

from the other two groups. The P29–37 group showed 66.98% effective stimulation sites, whereas the P17–28 and P38 and above groups showed 47% and 45%, respectively. At the range of 400–600 μm, the P29–37 group also had a significantly higher percentage value (40%) than the P17–28 (11.57%) and P38 and above (14.88%) groups. At a distance of >600 μm, the percentage value of the P38 and beyond group was significantly higher than those of the P17–28 and P29–37 groups. These results suggest that inhibitory connections undergo a constructive phase that peaks at around the

Table 1 Mean amplitude of evoked IPSCs following photo-stimulation. Amplitude was pooled from each 200-μm annulus from animals of the same age group

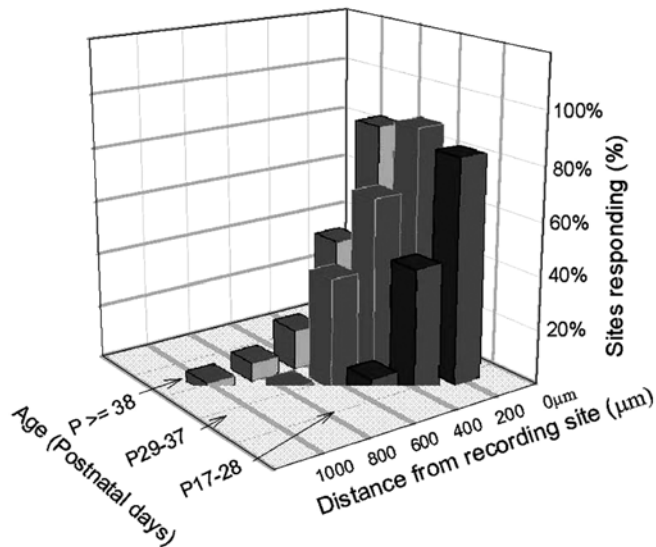| Postnatal age	Amplitude (pA) ± SD				
	<200 μm	200–400 μm	400–600 μm	600–800 μm	>800 μm
P17–28	7.34±2.45	5.46±2.12	4.53±1.76	NA	NA
P29–37	12.94±4.89	7.64±2.98	5.97±2.33	5.66±1.67	4.69±1.10
P38+	17.84±7.15	13.05±5.06	6.89±2.58	5.71±1.49	5.34±1.23

Table 2 Normalized evoked inhibitory input values for each 200-μm annulus of each age group (see Materials and methods for calculation method)

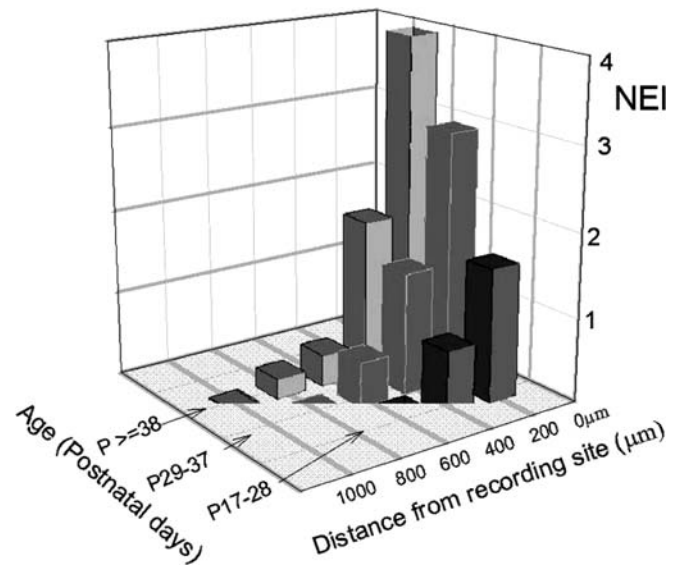| Postnatal age	NEI				
	<200 μm	200–400 μm	400–600 μm	600–800 μm	>800 μm
P17–28	1.59±0.23	0.77±0.02	0.16±0.01		
P29–37	3.00±0.31	1.45±0.13	0.53±0.02	0.07±0.005	0.03±0.004
P38+	4.56±0.42	1.87±0.18	0.45±0.02	0.24±0.01	0.14±0.005

period of eye opening. They are subsequently rearranged/ modified as the animals become more mature.

The normalized amplitude values (NEI, see Materials and methods) of IPSCs for each age group are shown in Table 2 and displayed as a histogram in Fig. 10. For all distances, the NEI values increased with increasing age, except in the 400- to 600-µm distance range, where no significant difference was found between the P29–37 and ≥P38 groups. In addition, for all age groups, the NEI values were highest close to the cell body and decreased with increasing distance from the cell body.

IPSC amplitudes increased with age; however, their time course also shortened, which may result from developmental changes in GABA_A receptor properties (Heinen et al. 2004). We have therefore calculated the total IPSC charge transfer for all age groups to account for the change in IPSC efficacy (Fig. 11). Charge transfer increases dramatically around eye opening (P30–P35). In addition, a second significant increase occurs between P40 and adulthood, indicating further strengthening of GA-BAergic connections. This increase was observed in all distance ranges but was most prominent in local connections (0–400 µm).

Fig. 10 Normalized inhibitory input (NEI) values calculated for each 200-µm distance range for each age group. Within-group comparison showed significant differences between each 200-µm range (P<0.05). Comparisons between age groups revealed significant differences between each age group for each 200-µm range (P<0.05), except at 400–600 µm, at which no significant difference was found between P29–37 and ≥P38 groups
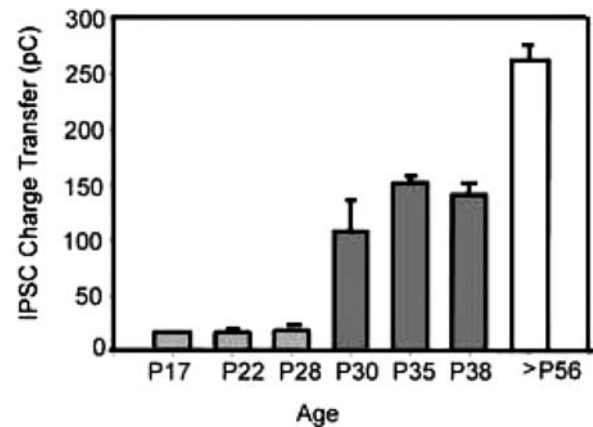
Fig. 11 Increase in mean IPSC charge transfer during postnatal development. A steep increase occurred around eye opening (P30–35) and between P40 and adulthood. Intracortical inhibition increases during the period of experience-driven remodeling and refinement of connections and reaches its highest, mature level when critical periods for refinement of maps and synaptic connections are closed. Bars represent mean and standard error; between 78 and 260 evoked synaptic events have been analyzed per age group

Discussion

The present study investigated the spatial pattern of inhibitory connections in the developing visual cortex. In light of the extreme functional importance of inhibitory connections, this is an important aspect of cortical circuit development, which has not been addressed before. Using the technique of photostimulation in combination with patch clamp recording, we have examined the spatial pattern of inhibitory inputs to pyramidal neurons in layers 2/3 of developing ferret striate cortex. Our results indicate

Fig. 9 Developmental changes in the origin of inhibitory synaptic inputs with regard to their distance from the target cell body. The percentage of effective stimulation sites (those that generate IPSCs in response to photostimulation) at a distance of 200 µm from each pyramidal neuron within each corresponding age group is shown. For within-group comparison, the percentages of IPSCs found at 0–200, 200–400, and 400–600 µm were significantly different from each other (P<0.02). Within the P29–37 group, the percentage of IPSCs found at 400–600 µm was significantly different from that found at 600 through 1,000 µm. For between-group comparison, the P28–37 group differed significantly from the P17–27 and ≥P38 groups at 200–400 and 400–600 µm (P<0.05). The ≥P38 group differed significantly from the other groups at >600 µm (P<0.02). All significance tests were done using one-way ANOVA and the Bonferroni t test

that the spatial pattern of intracortical inhibitory connections undergoes developmental rearrangements or modifications that coincide with developmental stages and events, such as eye opening and the initial presence and maturation of orientation maps.
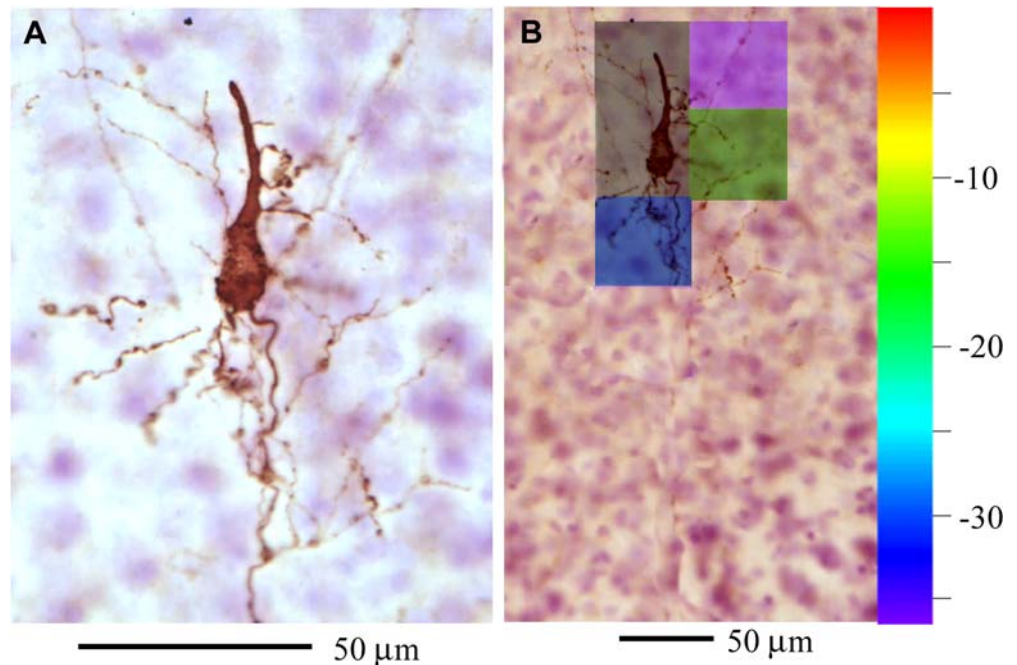
Methodological considerations

Slice preparation

The aim of this study was to analyze the development of inhibitory connections and their spatial arrangement since these parameters are of crucial importance to the development of functional response properties. We therefore made a strong effort to confine recording and stimulation sites to the upper cortical layers in tangential slices. However, owing to the curvature of the cortex we cannot completely rule out that some slices contained parts of other layers and that some intralaminar connections may have been stimulated. Although this potential problem may have contaminated some of our developmental results, the cresyl violet control stains and biocytin fills of recorded cells showed that the majority of recording sites and stimulation sites were in the upper layers.

Spatial resolution of the photostimulation method

The spatial extent of activated neurons around the laser spot is dependent on many factors, including the caged glutamate kinetic profile (in particular, its concentration over time), the laser flashing time, and the extent of dendritic trees in the surrounding neurons. Not all of these factors can be determined and, thus, spatial resolution had to be tested empirically in our system.

We performed voltage clamp in cell-attached mode on three pyramidal neurons (one from P28, two from P48). The Ca^{2+} concentration in bath solution was reduced to block synaptic transmission ("low calcium" in mM: 0.4 $CaCl_2$, 4.0 $MgSO_4$, all other ion concentrations were the same as in normal ACSF). One example is shown in Fig. 12. As is evident from the photostimulation map, spiking of the recorded neurons occurred only when its soma or proximal dendrites were directly stimulated. Activation of distal dendrites only elicited direct activation and no response was elicited when uncaging occurred immediately adjacent to the recorded neurons. This was observed for all three neurons tested. Indeed, recording under normal conditions also showed that spiking or direct activation could only be elicited from one or two locations directly under the recording pipette. In view of these observations, it appears that the effective stimulation area in the horizontal plane is at most less than 100 μm × 100 μm. We believe that this level of resolution suffices for the purpose of comparison between different age groups. This is under the assumption that if there was over- or underestimation of the spatial resolution, it occurred in all the cells that were recorded under the same condition.

Polysynaptic responses

Polysynaptic responses could occur if a glutamate-activated excitatory neuron elicited spiking of its target interneuron, which in turn projected to the recorded neuron. This seems unlikely because, as mentioned earlier, we never observed firing of recorded neurons by photostimulation of their presynaptic inputs. Spiking was only seen when the recorded neurons were directly stimulated. This occurred also in cell-attached mode with normal bath Ca^{2+} concentration. In the visual cortex,

Fig. 12 A Morphology of a pyramidal neuron tested in cell-attached mode. Ca^{2+} in bath solution was reduced to block synaptic transmission. **B** "Map" of evoked currents recorded from this cell. Spiking (*black color*) of the cell occurred when the laser spot hit the soma or proximal dendrites. Activation of distal dendrites only elicited direction (*other colors*). No response was observed when areas immediately adjacent to the cell were activated

extracellular recording in slice preparations also showed that action potentials could only be elicited when the recorded neuron was directly stimulated by the laser beam (Katz and Dalva 1994). In addition, we observed very little jitter in the response latencies upon repetitive stimulation of the same input, which is indicative of a monosynaptic connection. The length of the latency can be explained in part by the duration of uncaging and the concentration built up at the stimulation site. It should also be noted that the uncaging time for the more stable Nmoc-caged glutamate is longer than for commercially available compounds (see Rossi et al. 1997). However, the most critical factor is the time of spike generation in the presynaptic neuron. Once a spike has been generated, the remaining latency component is only determined by action potential propagation time and synaptic delay. If the spike occurs late following the laser flash (which we frequently observed by directly stimulating neurons while recording spikes in current clamp mode), the overall latency will be long. Response latencies of 40–100 ms or longer have, furthermore, been observed by other authors using the photostimulation techniques [e.g. Sawatari and Callaway 2000; Dantzker and Callaway 2000; Shepherd et al. 2003)].

Are spatial patterns of inputs at different ages merely the reflection of brain growth?

It is not likely that the disparate spatial patterns for different age groups are the result of cell density change as brain grows. If this were the case, we would expect the density of local inputs to be decreased in more mature animals. However, our results indicated that the percentage of local inputs (200 µm) did not differ significantly among the three groups examined (Fig. 9).

Source of inhibition

Application of GABAzine to the bath solution almost abolished the IPSCs that occurred before 100 ms (Fig. 2C). Therefore, it is assumed that the IPSCs recorded resulted mostly from activation of $GABA_A$ receptors. The slow, G-protein-coupled, metabotropic $GABA_B$ receptor has been reported to be involved in shaping the response properties of individual neurons (Allison 1996). However, this component was difficult to measure in our study because whole-cell patch clamp recording dialyzes second messenger compounds out of neurons.

Late development of inhibitory connections

IPSCs were only occasionally observed in the youngest age group (P7–16). Their amplitude was also small (<8 pA). Their paucity prevented us from generalizing a spatial input pattern. Anatomically, however, it has been shown that bands of GABA-reactive neurons are present at cortical and subcortical plates of ferrets as early as the first postnatal day (Gao et al. 1999). Functional GABAergic synaptic connection in neonatal mouse barrel cortex has also been reported (Agmon et al. 1996). The paucity of IPSCs in our study could have been due to the following factors:

1. Our current detection threshold is not sensitive enough to detect the IPSCs. This seems unlikely, however, since we did detect IPSCs in some slice preparation in this age group. In addition, EPSCs were observed in all the recorded neurons.
2. Inhibitory synapses in young animals have a more depolarized potential, owing to a higher intracellular chloride concentration. At a holding potential of –20 mV, the driving force could have been too small to elicit any IPSCs. We did not directly test this possibility. However, again, we did observe IPSCs in some cases within this age group.
3. It has been shown that inhibitory inputs in newborn animals originate only locally (Agmon et al. 1996). It is possible that these local IPSCs were masked by direct activation currents that resulted from stimulation of dendritic arborization of the recorded neurons. However, local IPSCs in more mature age groups were easily detected. Therefore, this assumption holds under the condition that IPSCs in young animals are of very small amplitude.
4. Inhibitory neurons in young animals could be less sensitive to glutamate, and thus less excitable. The immaturity of inhibitory interneurons could explain the paucity of IPSCs observed in our study. These neurons are less excitable by other neurons and thus exert less inhibitory effect on their target neurons. The fact that IPSCs were detected in newborn mice but not in ferrets until P17 could have been due to species differences. Unlike monkeys, cats, rats, and mice, ferrets are born before thalamocortical inputs reach the subplate and well before development of the cortical plate is complete (Luskin and Shatz 1985).

The first discernible pattern of inhibitory inputs was present at around P17 (Fig. 6A), which is at least more than 1 week later than the initial appearance of excitatory connections (Dalva and Katz 1994). The late presence of functional inhibition in this study is consistent with other reports (Komatsu and Iwakiri 1991; Luhmann and Prince 1991; Gao et al. 1999) that the development of intracortical inhibitory circuits lags behind that of the excitatory ones. This could partly account for the observation that visual cortical neurons respond to visual stimulation but lack selective responsiveness in newborn animals (Blakemore and Van Sluyters 1975; Buisseret and Imbert 1976). It could also be responsible for the critical time window during which the organization of intracortical circuitry can be strongly influenced by sensory experience (Kirkwood et al. 1997; Micheva and Beaulieu 1997).

Development of inhibitory connections is related to the refinement of response properties in the visual cortex

In adult animals, the intracortical inhibitory circuits are believed to play a major role in shaping the orientation selectivity of cortical neurons (Sillito 1979; Woergoetter and Koch 1991; Berman et al. 1991; Somers et al. 1995; Roerig and Chen 2002). In ferret visual cortex, orientation tuning could be recorded as early as P23 by single-unit recording (Chapman and Stryker 1993) and at P31–36 by optical imaging (Chapman et al. 1996). The latter technique is less sensitive and thus requires stronger underlying intrinsic signal. This time frame corresponds to our observations that inhibitory connection was in the early immature stage at P23 and in the peak of its construction phase around eye opening. The low-contrast initial orientation map matures into an adult-like, high-contrast map at around P39 (Chapman et al. 1996). Our data show that the spatial pattern of inhibitory connections at P38 resembled that of adult animals. At this developmental age, the vast majority of inhibitory inputs originated from immediate areas close to the recorded neurons (200–300 μm). This is consistent with the anatomical organization of dense local axonal collaterals of inhibitory neurons found within layer 2/3 (Beaulieu and Somogyi 1990; Kisvarday et al. 1993). The number of relatively distant inputs (300–600 μm), which were abundant around the period of eye opening, was sharply reduced. Thus, it appears that a smaller, but focused and stronger (i.e., bigger IPSC amplitude) inhibitory input source is essential for cortical neuron feature selectivity.

Chronic cortical optical imaging in developing ferrets indicates that the structure of orientation maps, including the locations of orientation domains, remains remarkably constant during development (Chapman et al. 1996). This implies that the orientation feature selectivity is predefined early in the development and is experience independent (Chapman et al. 1996, Goedecke and Bonhoeffer 1996). The selectivity could well be the product of interplay between excitatory and inhibitory connections during development. Similar to inhibitory connections, excitatory inputs undergo a constructive phase that peaks around or shortly after eye opening (Dalva and Katz 1994). At this period, both the local excitatory and the local inhibitory inputs reach their maximum numbers. As described above, it is at this time that the primitive orientation map is first detected, and it remains relatively unchanged later in normal development (Chapman et al. 1996). Therefore, it is assumed that a primitive excitatory and inhibitory framework has been formed at this period. Its components are subject to modification by substitution, deletion, and insertion commensurate with visual experience. Following subsequent normal development, the relative number of local excitatory inputs declines whereas that of inhibitory inputs increases. This is accompanied by the sharpening of orientation tuning. Thus, it appears that a balance between the relative numbers of local excitatory versus inhibitory inputs affects orientation tuning.

References

Agmon A, Hollrigel G, O'Dowd DK (1996) Functional GABAergic synaptic connection in neonatal mouse barrel cortex. J Neurosci 16:4684–4695

Albus K, Wahle P (1994) The topography of tangential inhibitory connections in the postnatally developing and mature striate cortex of the cat. Eur J Neurosci 6:779–792

Albus K, Wahle P, Lubke J, Matute C (1991) The contribution of GABA-ergic neurons to horizontal intrinsic connections in upper layers of the cat's striate cortex. Exp Brain Res 85:235–239

Allison JD, Kabara JF, Snider RK, Casagrande VA, Bonds AB (1996) GABAB-receptor-mediated inhibition reduces the orientation selectivity of the sustained response of striate cortical neurons in cats. Vis Neurosci 13:559–566

Azouz R, Gray CM, Nowak LG, McCormick DA (1997) Physiological properties of inhibitory interneurons in cat striate cortex. Cereb Cortex 7:534–545

Beaulieu C, Somogyi P (1990) Targets and quantitative distribution of GABAergic synapses in the visual cortex of the cat. Eur J Neurosci 2:296–303

Berman NJ, Douglas RJ, Martin KA, Whitteridge D (1991) Mechanisms of inhibition in cat visual cortex. J Physiol 440:667–722

Berman NJ, Douglas RJ, Martin KAC (1992) GABA-mediated inhibition in the neural networks of visual cortex. Prog Brain Res 90:443–476

Blakemore C, Van Sluyters RC (1975) Innate and environmental factors in the development of kitten's visual cortex. J Physiol 248:663–716

Blue ME, Parnavelas JG (1983) The formation and maturation of synapses in the visual cortex of the rat. II. Quantitative analysis. J Neurocytol 12:697–712

Bonhoeffer T, Grinvald A (1991) Iso-orientation domains in cat visual cortex are arranged in pinwheel like patterns. Nature 353:429–431

Buisseret P, Imbert M (1976) Cortical cells: their developmental properties in normal and dark reared kittens. J Physiol 255:511–525

Callaway EM, Katz LC (1990) Emergence and refinement of clustered horizontal connections in cat striate cortex. J Neurosci 10:1134–1153

Callaway EM, Katz LC (1993) Photostimulation using caged glutamate reveals functional circuitry in living brain slices. Proc Natl Acad Sci U S A 90:7661–7665

Chapman B, Stryker MP (1992) Origin of orientation tuning in the visual cortex. Curr Opin Neurobiol 2:498–501

Chapman B, Stryker MP (1993) Development of orientation selectivity in ferret visual cortex and effects of deprivation. J Neurosci 13:5251–5262

Chapman B, Stryker MP, Bonhoeffer T (1996) Development of orientation preference maps in ferret primary visual cortex. J Neurosci 16:6443–6453

Crook JM, Eysel UT, Machemer HF (1991) Influence of GABA-induced remote inactivation on the orientation tuning of cells in area 18 of feline visual cortex: a comparison with area 17. Neuroscience 40:1–12

Crook JM, Kisvarday ZF, Eysel UT (1997) GABA-induced inactivation of functionally characterized sites in cat striate cortex: effects on orientation tuning and direction selectivity. Vis Neurosci 14:141–158

Dalva MB, Katz LC (1994) Rearrangements of synaptic connections in visual cortex revealed by laser photostimulation. Science 265:255–258

Dalva MB, Weliky M, Katz LC (1997) Relationships between local synaptic connections and orientation domains in primary visual cortex. Neuron 19:871–880

Dantzker JL, Callaway EM (2000) Laminar sources of synaptic input to cortical inhibitory interneurons and pyramidal neurons. Nat Neurosci 3:701–7

Eysel UT (1992) Lateral inhibitory interactions in areas 17 and 18 of the cat visual cortex. Prog Brain Res 90:407–422

Eysel UT, Muche T, Worgotter F (1988) Lateral interactions at direction-selective striate neurones in the cat demonstrated by local cortical inactivation. J Physiol 399:657–675

Eysel UT, Crook JM, Machemer HF (1990) GABA-induced remote inactivation reveals cross-orientation inhibition in the cat striate cortex. Exp Brain Res 80:626–630

Ferster D, Chung S, Wheat HS (1996) Orientation selectivity of thalamic input to simple cells of cat visual cortex. Nature 380:249–252

Gao WJ, Newman DE, Wormington AB, Pallas SL (1999) Development of inhibitory circuitry in visual and auditory cortex of postnatal ferrets: immunocytochemical localization of GABAergic neurons. J Comp Neurol 409:261–273

Gibber M, Chen B, Roerig B (2001) Direction selectivity of excitatory and inhibitory neurons in ferret visual cortex. Neuroreport 12:2293–2296

Goedecke I, Bonhoeffer T (1996) Development of identical orientation maps for two eyes without common visual experience. Nature 379:251–254

Heggelund P (1981) Receptive field organization of simple cells in cat striate cortex. Exp Brain Res 42:89–98

Heinen K, Bosman LW, Spijker S, Van Pelt J, Smit AB, Voorn P, Baker RE, Brussaard AB (2004) GABA(a) receptor maturation in relation to eye opening in the rat visual cortex. Neuroscience124:161–171

Hensch TK, Fagiolini M, Mataga N, Stryker MP, Baekkeskov S, Kash SF (1998) Local GABA circuit control of experience-dependent plasticity in developing visual cortex. Science 282:1504–1508

Huang ZJ, Kirkwood A, Pizzorusso T, Porciatti V, Morales B, Bear MF, Maffei L, Tonegawa S (1999) BDNF regulates the maturation of inhibition and the critical period of plasticity in mouse visual cortex. Cell 98:739–755

Hubel DH, Wiesel TN (1962) Receptive fields, binocular interactions and functional architecture in the cat's visual cortex. J. Physiol (Lond) 160:106–154

Hubel DH, Wiesel TN (1963) Shape and arrangement of columns in cat's striate cortex. J. Physiol (Lond) 165:559–568

Katz LC, Dalva MB (1994) Scanning photostimulation: a new approach for analyzing brain circuits. J Neurosci Methods 54:205–218

Kawaguchi Y, Kubota Y (1997) GABAergic cell subtypes and their synaptic connections in rat frontal cortex. Cereb Cortex 6:476–486

Kim G, Kandler K (2003) Elimination and strengthening of glycinergic/GABAergic connections during tonotopic map formation. Nat Neurosci 6:282–290

Kirkwood A, Bear MF (1994) Hebbian synapses in visual cortex. J Neurosci 14:1634–1635

Kirkwood A, Silva A, Bear MF (1997) Age-dependent decrease of synaptic plasticity in the neocortex of αCaMkII mutant mice. Proc Natl Acad Sci U S A 94:3380–3383

Kisvarday ZF (1992) GABAergic networks of basket cells in the visual cortex. Prog Brain Res 90:385–405

Kisvarday ZF, Beaulieu C, Eysel UT (1993) Network of GABAergic large basket cells in cat visual cortex (area 18): implication for lateral disinhibition. J Comp Neurol 327:398–415

Komatsu Y, Iwakiri M (1991) Postnatal development of neuronal connections in cat visual cortex studied by intracellular recording in slice preparation. Brain Res 540:14–24

Kritzer MF, Cowey A, Somogyi P (1992) Patterns of inter- and intralaminar GABAergic connections distinguish striate (V1) and extrastriate (V2, V4) visual cortices: their functionally specialized subdivisions in the rhesus monkey. J Neurosci 12:4545–4564

Lubke J, Albus K (1992) Rapid rearrangement of intrinsic tangential connections in the striate cortex of normal and dark-reared kittens: lack of exuberance beyond the second postnatal week. J Comp Neurol 323:42–58

Luhmann HJ, Prince DA (1991) Postnatal maturation of GABAergic system in rat neocortex. J Neurophysiol 65:247–263

Luskin MB, Shatz CJ (1985) Neurogenesis of the cat's primary visual cortex. J Comp Neurol 242:611–631

Martin KAC (1988) From single cells to simple circuits in the cerebral cortex. Q J Exp Physiol 73:637–702

Micheva KD, Beaulieu C (1997) Development and plasticity of the inhibitory neocortical circuitry with an emphasis on the rodent barrel field cortex: a review. Can J Physiol Pharmacol 75:470–478

Miller MW (1986) The migration and neurochemical differentiation of gamma-aminobutyric acid (GABA)-immunoreactive neurons in rat visual cortex as demonstrated by a combined immuno-cytochemical–autoradiographic technique. Brain Res 1:41–46

Rittenhouse CD, Shouval HZ, Paradiso MA, Bear MF (1999) Monocular deprivation induces homosynaptic long-term depression in visual cortex. Nature 397:347–350

Rockland KS. Lund JS. Humphrey AL (1982) Anatomical binding of intrinsic connections in striate cortex of tree shrews (*Tupaia glis*). J Comp Neurol 209:41–58

Roerig B, Chen B (2002) Relationships of local inhibitory and excitatory circuits to orientation preference maps in ferret visual cortex. Cereb Cortex 12:187–198

Roerig B, Kao JP (1999) Organization of intracortical circuits in relation to direction preference maps in ferret visual cortex. J Neurosci 1999 19(24):RC44

Rossi FM, Margulis M, Tang CM, Kao JP (1997) N-Nmoc-L-glutamate, a new caged glutamate with high chemical stability and low pre-photolysis activity. J Biol Chem 272:32933–32939

Sanes DH, Takacs C (2003) Activity-dependent refinement of inhibitory connections. Eur J Neurosci 6:570–574

Sawatari A, Callaway EM (2000) Diversity and cell type specificity of local excitatory connections to neurons in layer 3B of monkey primary visual cortex. Neuron 2:459–471

Shepherd GM, Pologruto TA, Svoboda K (2003) Circuit analysis of experience-dependent plasticity in the developing rat barrel cortex. Neuron 38:277–298

Shmuel A, Grinvald A (1996) Functional organization for direction of motion and its relationship to orientation maps in cat area 18. J Neurosci 16:6945–6964

Sillito AM (1979) Inhibitory mechanisms influencing complex cell orientation selectivity and their modification at high resting discharge levels. J Physiol 289:33–53

Sillito AM (1984) Functional considerations of the operation of GABAergic inhibitory processes in the visual cortex. In: Jones EG, Peters A (eds) Cerebral cortex, vol 2. Plenum Press, New York, pp 91–117

Sillito AM, Kemp JA, Milson JA, Berardi N (1980) A reevaluation of the mechanisms underlying simple cell organization selectivity. Brain Res 194:517–520

Somers DC, Nelson SB, Sur M (1995) An emergent model of orientation selectivity in cat visual cortical simple cells. J Neurosci 15:5448–5465

Vidyasagar TR, Pei X, Volgushev M (1996) Multiple mechanisms underlying the orientation selectivity of visual cortical neurons. Trends Neurosci 19:272–277

Weliky M, Bosking WH, Fitzpatrick D (1996) A systematic map of direction preference in primary visual cortex. Nature 379:725–728

Winfield DA. The postnatal development of synapses in the different laminae of the visual cortex in the normal kitten and in kittens with eyelid suture. Brain Res 285:155–169

Woergoetter F, Koch C (1991) A detailed model of the primary visual pathway in the cat: comparison of afferent excitatory and intracortical inhibitory connection schemes for orientation selectivity. J Neurosci 11:1959–1979